J. Biomed. Eng. Res : 279-287, 2009

CoReHA: conductivity reconstructor using harmonic algorithms for magnetic resonance electrical impedance tomography (MREIT)

Kiwan Jeon[1], Chang-Ock Lee[1], Hyung Joong Kim[2], Eung Je Woo[2], Jin Keun Seo[3]

[1]*Department of Mathematical Sciences, KAIST, Daejeon, Korea*
[2]*College of Electronics and Information, Kyung Hee University, Gyeonggi-do, Korea*
[3]*Department of Mathematics, Yonsei University, Seoul, Korea*
(Received April 20, 2009. Accepted June 18, 2009)

Abstract

Magnetic resonance electrical impedance tomography (MREIT) is a new medical imaging modality providing cross-sectional images of a conductivity distribution inside an electrically conducting object. MREIT has rapidly progressed in its theory, algorithm and experimental technique and now reached the stage of *in vivo* animal and human experiments. Conductivity image reconstructions in MREIT require various steps of carefully implemented numerical computations. To facilitate MREIT research, there is a pressing need for an MREIT software package with an efficient user interface. In this paper, we present an example of such a software, called CoReHA which stands for conductivity reconstructor using harmonic algorithms. It offers various computational tools including preprocessing of MREIT data, identification of boundary geometry, electrode modeling, meshing and implementation of the finite element method. Conductivity image reconstruction methods based on the harmonic B_z algorithm are used to produce cross-sectional conductivity images. After summarizing basics of MREIT theory and experimental method, we describe technical details of each data processing task for conductivity image reconstructions. We pay attention to pitfalls and cautions in their numerical implementations. The presented software will be useful to researchers in the field of MREIT for simulation as well as experimental studies.

Key words : magnetic resonance electrical impedance tomography, conductivity image, conductivity reconstructor using harmonic algorithms

I. INTRODUCTION

A new bio-imaging modality called magnetic resonance electrical impedance tomography (MREIT) has been lately introduced, which allows high-resolution tomographic imaging of a conductivity distribution inside an electrically conducting object [1-7]. MREIT utilizes an MRI scanner as a tool to measure a magnetic flux density distribution inside an imaging object induced by an externally injected current. A nonlinear relationship between the measured magnetic flux density and the conductivity provides the fundamental basis of the image reconstruction problem in MREIT. Following numerous studies on its theory, algorithm and experimental technique, it has now reached the stage of *in vivo* animal and human experiments [8,9]. The most challenging technical problem to be addressed in near future is how to reduce the amount of injection current to an acceptable level without deteriorating the image quality. This demands more advanced MREIT research including innovative data collection schemes and improved data processing methods. In this paper, we deal with such data processing methods.

Conductivity image reconstructions in MREIT require a series of data processing tasks including k-space MR data handling, Fourier transformation, phase unwrapping, image segmentation, meshing, denoising, numerical solution of a partial differential equation and various other computations. To ensure the efficacy of ongoing and future MREIT studies, we should be well equipped with a versatile MREIT software package that includes not only numerical implementations of these tasks but computer graphics for image visualization, graphical user interface, data management and others.

Recognizing a need for such a software package, Kim *et al.* developed an MREIT toolbox for Matlab (Mathworks, Inc.,

Corresponding Author : Eung Je Woo
Department of Biomedical Engineering, College of Electronics and Information, Kyung Hee Univ.
1 Seochun, Giheung, Yongin, Gyeonggi, 446-701, Korea
Tel : +82-31-201-2538 / Fax : +82-31-201-2378
E-mail : ejwoo@khu.ac.kr
This work was supported by the Korea Science and Engineering Foundation (KOSEF) grant funded by the Korea government (MEST) (R11-2002-103). Chang-Ock Lee and Jin Keun Seo were supported by KRF-2006-311-C00015.

MA, USA) [10]. Its use has been, however, limited to the developers primarily due to difficulties in both understanding how it works and learning how to use it. Recent advancements in MREIT theory and algorithm also impose necessary updates of the previously developed toolbox.

To facilitate multilateral studies in the future, we have developed a new MREIT software package to be distributed together with test data sets. Emphasizing the ease of use, we have designed the software as an application program for the Microsoft Windows operating system (Microsoft, WA, USA). Incorporating outcomes of the latest MREIT research, the software named as CoReHA (Conductivity Reconstructor using Harmonic Algorithms) provides all the data processing routines needed to produce multi-slice conductivity images from measured k-space MR data sets. In terms of the image reconstruction algorithm, CoReHA currently supports only the harmonic B_z algorithm [11,12] and the local harmonic B_z algorithm [13]. As summarized in the review paper by Woo and Seo [7], there are several other algorithms that may be included in the next version of CoReHA. Related with the data collection strategy, CoReHA deals with the so called B_z -based MREIT [14] where only the z-directional component of the induced magnetic flux density is measured and utilized in the conductivity image reconstruction. In this paper, z axis points to the direction of the main magnetic field of the MRI scanner used in MREIT experiments.

CoReHA is available from the website *http://iirc.khu.ac.kr* with its manual. The primary goal of this paper is to provide all the necessary technical information to understand how CoReHA works. We briefly review the basic theory, experimental process and image reconstruction algorithm. Identifying necessary data processing tasks, we will explain their numerical implementations and necessary cautions. Wrapping up the description on CoReHA, we will demonstrate the conductivity image reconstruction process using typical data sets from recent animal imaging experiments. At the end, we will discuss our plans for the next version of CoReHA.

II. CONDUCTIVITY IMAGING IN MREIT USING HARMONIC B_z ALGORITHM

A. Basics of MREIT

We assume a three-dimensional imaging object Ω with its conductivity distribution σ and boundary $\partial\Omega$. Attaching a pair of surface electrodes, we inject low-frequency current I into the object. Injected current spreads throughout the domain Ω and induces distributions of current density **J**, voltage u and magnetic flux density **B**. These are determined by the conductivity distribution σ and boundary geometry of the imaging object as well as the electrode configuration.

The induced voltage u in Ω satisfies the following boundary value problem with the Neumann boundary condition:

$$\begin{cases} \nabla \cdot (\sigma(r)\nabla u(r)) = 0 \ \text{ in } \ \Omega \\ -\sigma\nabla u \cdot n = g \ \text{ on } \ \partial\Omega \end{cases} \tag{1}$$

where **n** is the outward unit normal vector on $\partial\Omega$, g is a normal component of the current density on $\partial\Omega$ due to I and **r** is a position vector in R^3. The current density **J** is given by

$$J(r) = -\sigma(r)\nabla u(r) \ \text{ in } \ \Omega \tag{2}$$

The induced magnetic flux density **B** in Ω can be expressed as

$$B(r) = B_\Omega(r) + B_{x(r)} \ \text{ in } \ \Omega \tag{3}$$

where B_Ω is the magnetic flux density due to **J** in Ω and B_x is from currents in lead wires and surfaces of electrodes. From the Biot-Savart law,

$$B_\Omega(r) = \frac{\mu_0}{4\pi}\int_\Omega J(r')\times\frac{r-r'}{|r-r'|^3}dr' \tag{4}$$

Lee *et al.* investigated the term B_x and suggested experimental and also algorithmic ways of minimizing its effects [15]. In this paper, we will assume that $B = B_\Omega$.

In the B_z-based MREIT, we measure only B_z using an MRI scanner. Extracting the z-component from (4), we can see that B_z is related with σ as

$$B_z(r) = \frac{\mu_0}{4\pi}\int_\Omega \frac{(x'-x)J_y(r') - (y'-y)J_x(r')}{|r-r'|^3}dr' \tag{5}$$

or

$$B_z(r) = \frac{\mu_0}{4\pi}\int_\Omega \frac{\sigma(r)\left[(x-x')\frac{\partial u}{\partial y}(r') - (y-y')\frac{\partial u}{\partial x}(r')\right]}{|r-r'|^3}dr' \tag{6}$$

From the Ampere law, J in (2) can be expressed as

$$J(r) = \frac{1}{\mu_0}\nabla\times B(r) \ \text{ in } \ \Omega \tag{7}$$

Since we are dealing with the externally injected current with no internal source or sink of the same kind, we have

$$\nabla \cdot J(r) = \frac{1}{\mu_0} \nabla \cdot \nabla \times B(r) = 0 \text{ in } \Omega \qquad (8)$$

In MREIT, we generate an image of σ from measured B_z data based on relations from (1) to (8). More details on the basic theory can be bound in the recent review paper [7].

B. Imaging experiment

As shown in Figure 1(a), we attach two pairs of surface electrodes $\{\varepsilon_1^+, \varepsilon_1^-\}$ and $\{\varepsilon_2^+, \varepsilon_2^-\}$ around a chosen imaging region or segment of the object. This allows us to inject currents along two different directions, the first current I_1 between ε_1^+ and ε_1^- and the second current I_2 between ε_2^+ and ε_2^-. For an isotropic (or equivalent isotropic) conductivity image reconstruction [8,9], we get induced magnetic flux densities $B_{z,1}$ and $B_{z,2}$ corresponding to I_1 and I_2, respectively. Recent experimental studies suggest two pairs of thin and flexible carbon-hydrogel electrodes covering as much surface area of the imaging region as possible [7]. For the injection of these currents, we need a constant current source that is synchronized with a spectrometer of an MRI scanner [16].

Inside the bore of the MRI scanner, we place the imaging object with four electrodes attached around the chosen imaging region. Injecting current I_1 from ε_1^+ to ε_1^-, we collect a set of k-space data S_1^+. Switching ε_1^+ and ε_1^-, we inject -I_1 and collect another set of k-space data S_1^-. We repeat these for I_2 along the other orthogonal direction between ε_2^+ and ε_2^- to get k-space data sets S_2^+ and S_2^-. From these k-space data, we extract induced magnetic flux density data $B_{z,1}$ and $B_{z,2}$ subject to I_1 and I_2, respectively. In this paper, we skip other technical details of MREIT imaging experiments including shimming, RF coil, pulse sequence, artifact removal, noise estimation and so on.

C. Harmonic B_z algorithm

In the harmonic B_z algorithm [11,12], we utilize $B_{z,1}$ and $B_{z,2}$ to produce an image of σ using the following identity:

$$\begin{bmatrix} \frac{\partial \ln\sigma}{\partial x}(r) \\ \frac{\partial \ln\sigma}{\partial y}(r) \end{bmatrix} = \frac{1}{\mu_0}(A[\sigma](r))^{-1} \begin{bmatrix} \nabla^2 B_{z,1}(r) \\ \nabla^2 B_{z,2}(r) \end{bmatrix}, \quad r \in \Omega \qquad (9)$$

where

$$A[\sigma](r) = \begin{bmatrix} \sigma\frac{\partial u_1[\sigma]}{\partial y}(r) & -\sigma\frac{\partial u_1[\sigma]}{\partial x}(r) \\ \sigma\frac{\partial u_2[\sigma]}{\partial y}(r) & -\sigma\frac{\partial u_2[\sigma]}{\partial x}(r) \end{bmatrix}, \quad r \in \Omega$$

and $u_j[\sigma]$ is an induced voltage subject to injection current I_j satisfying

$$\begin{cases} \nabla \cdot (\sigma \nabla u_j[\sigma]) = 0 \ \in \ \Omega, \\ I = \int_{\varepsilon_j^+} \sigma\frac{\partial u_j[\sigma]}{\partial n} ds = -\int_{\varepsilon_j^-} \sigma\frac{\partial u_j[\sigma]}{\partial n} ds, \\ \nabla u_j[\sigma] \times n|_{\varepsilon_j^+ \cup \varepsilon_j^-} = 0, \\ \sigma\frac{\partial u_j[\sigma]}{\partial n} = 0 \text{ on } \partial\Omega \setminus \overline{\varepsilon_j^+ \cup \varepsilon_j^-} \end{cases} \qquad (10)$$

Here, **n** denotes the outward normal vector to $\partial\Omega$. We now summarize the conductivity image reconstruction procedure using the harmonic B_z algorithm.

It consists of the following six steps.

Step 0 Choose an MREIT pulse sequence and inject electrical currents I_1 and I_2 through pairs of surface electrodes $\varepsilon_1^\pm$ and $\varepsilon_2^\pm$, respectively, to get k-space data sets $S_1^\pm$ and $S_2^\pm$ using the MRI scanner.

Step 1 Produce an MR magnitude image M and induced magnetic flux densities B_z,j images for j = 1, 2

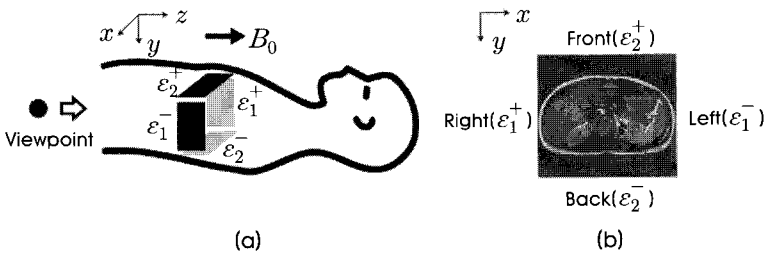

Fig. 1. (a) Experimental setup and (b) cross-sectional MR magnitude image of an imaging slice. Note the chosen coordinate system.

from the k-space data.

Step 2 Given the MR magnitude image M, perform segmentation of $\partial\Omega$ and $\varepsilon_j^{\pm}$ using an image segmentation method.

Step 3 Set an initial guess σ^0 in Ω, for example $\sigma^0 = 1$.

Step 4 For the given initial conductivity $\sigma = \sigma^0$, compute a numerical solution of (10).

Step 5 For a given slice $\Omega_{z0} = \Omega \cap \{z = z_0\}$, use the finite element method (FEM) to solve the two-dimensional Poisson equation

$$\left(\frac{\partial^2}{\partial x^2}+\frac{\partial^2}{\partial y^2}\right)\ln\sigma^1 = \nabla_{x,y} \cdot \left(A[\sigma^0]^{-1}\begin{bmatrix}\nabla^2 B_{z,1}\\ \nabla^2 B_{z,2}\end{bmatrix}\right) \in \Omega_z \quad (11)$$

with the Neumann boundary condition

$$\nabla_{x,y}\ln\sigma^1 \cdot v = \left(A[\sigma^0]^{-1}\begin{bmatrix}\nabla^2 B_{z,1}\\ \nabla^2 B_{z,2}\end{bmatrix}\right) \cdot v \text{ on } \partial\Omega_z, \quad (12)$$

where $\nabla_{x,y} = \left(\frac{\partial}{\partial x}, \frac{\partial}{\partial y}\right)$ and v is the two-dimensional outward normal vector to $\partial\Omega_z$.

Step 6 Scale σ^1 as

$$\sigma^1 \leftarrow \frac{u_1[\sigma^1]|\varepsilon_2^+ - u_1[\sigma^1]|\varepsilon_2^-}{V_1^+ - V_1^-}\sigma^1$$

where $V_1^+ - V_1^-$ is a measured voltage difference between electrodes ε_2^+ and ε_2^- subject to the injection current I_1. This step may be skipped if only the conductivity contrast is needed without absolute conductivity values in S/m. For most clinical applications, it is enough to find a scaled conductivity image instead of an absolute conductivity image since the image contrast is of primary concern.

Step 7 If necessary, repeat steps 3 to 6 with σ^1 in place of σ^0 to get an updated conductivity image σ^2. Iterate if the image quality is improved.

In the original harmonic B_z algorithm [11,12], steps 4 and 5 are repeated to get σ^n from σ^{n-1} until it converges. We found that such an iteration does not improve the image quality in most practical cases mainly due the presence of noise in measured B_z data. In CoReHA, we do not iterate and produce a scaled conductivity image σ^1 providing only a contrast information. For this purpose, we solve the following simplified problem in step 4 instead of (10) [13]:

$$\begin{cases}\nabla_{x,y} \cdot (\sigma\nabla_{x,y}u_j[\sigma]) = 0 \in \Omega_z\\ u_j = 1 \text{ on } \varepsilon_j^+ \cap \Omega_z\\ u_j = -1 \text{ on } \varepsilon_j^- \cap \Omega_z\\ \sigma\dfrac{\partial u_j[\sigma]}{\partial v} = 0 \text{ on } \partial\Omega_z \setminus \overline{\varepsilon_j^+ \cup \varepsilon_j^-}\end{cases} \quad (13)$$

In step 5, we also adopt the simplified boundary condition of

$$\sigma^1 = 1 \text{ on } \partial\Omega_z \quad (14)$$

to replace (12).

III. IMPLEMENTATION IN CoReHA

In this section, we describe details and cautions of each data processing task involved in MREIT conductivity image reconstructions. Numerical implementations of all the necessary tasks are not straight-forward and involve several innovative approaches. They cannot be handled through any readily available commercial or open software package.

CoReHA is designed as a user friendly software with graphical user interface (GUI) for those tasks. It is a Microsoft Windows application program developed by using the Visual C++ compiler, Microsoft Foundation Class Library (Microsoft, WA, USA) and OpenGL [17]. The key features are as follows:

- Computation of magnetic flux density data B_z from k-space data
- Geometrical modeling of imaging domain via segmentation and electrode modeling
- Denoising and harmonic inpainting
- Conductivity image reconstruction

Each part is accompanied by numerous graphical visualization and user interface tools to allow real-time feedback of outcomes at every step. In order to be independent of an MRI scanner, it might be better to begin with B_z data sets already obtained. We, however, choose k-space data sets as the starting point since we have found that getting B_z data from k-space data is nontrivial.

A. Magnitude image reconstruction and coordinate setting

There are two k-space data sets and each data set contains two k-space data $S_j^{\pm}(m, n, z)$ for $j = 1, 2$:

$$S_j^{\pm}(m, n, z) = \iint M(x, y, z)e^{i\delta(x,y,z)}e^{\pm i\gamma B_{zj}(x,y,z)T_c}e^{-i(xm\Delta k_x + yn\Delta k_y)}\,dxdy, \quad (15)$$

where M is a conventional MR magnitude image, δ any systematic phase artifact, $\gamma = 26.75 \times 10^7\,\mathrm{rad/Tesla} \cdot s$ the gyromagnetic ratio of hydrogen and T_c the current pulse width in seconds.

Applications of the discrete inverse Fourier transformation to (15) give the following complex images:

$$M_j^{\pm}(x,y,z) = M(x,y,z)e^{i\delta(x,y,z)}e^{\pm i\gamma B_{z,j}(x,y,z)T_c} \quad (16)$$

Taking the magnitude of either M_j^+ or M_j^-, we get multi-slice magnitude images $M(x,y,z)$ for $z = z_1, \cdots, z_K$ where K is the number of slices. In CoReHA, we use the well-known public library of the fast Fourier transformation, FFTW [18] for the discrete inverse Fourier transformation.

Orientation or coordinate of the image M depends on the ordering of k-space data including the consequence of a chosen specific pulse sequence. CoReHA displays multi-slice magnitude images of $M(x,y,z)$ for $z = z_1, \cdots, z_K$ and asks the user to set positive directions of x, y and z axes on the screen. Remembering the orientation of the images, CoReHA sets up a proper coordinate system for internal computations. When CoReHA is used for the first time with a certain MRI scanner and a chosen pulse sequence, one might need to use a phantom of which images can provide sufficient information about the image orientation.

B. Phase image reconstruction and extraction of B_z image

Dividing M^+ by M^- and taking its argument, we get a phase image Φ as

$$\Phi(x,y,z) = \arg\left(\frac{M^+(x,y,z)}{M^-(x,y,z)}\right) \quad (17)$$

The phase image Φ is wrapped in the range of $-\pi$ and $+\pi$ due to the branch cut of the argument operator. Since B_z is proportional to Φ and must be continuous, we unwrap Φ before converting it to B_z.

A simple phase unwrapping method fails catastrophically in the presence of noise due to the appearance of so-called phase singularities. In CoReHA, we use the Goldstein's algorithm whose source code is provided in the textbook by Ghiglia and Pritt [19]. Using a two-dimensional phase unwrapping operator, $\mathrm{unwrap}_{x,y}(\cdot)$, we can obtain $\widetilde{B_z}$ for a specific slice at $z = z_k$ as

$$\widetilde{B_z}(x,y,z_k) = \frac{1}{2\gamma T_c}\ \mathrm{unwrap}_{x,y}\ \Phi(x,y,z_k) \quad (18)$$

Since we unwrap $\Phi(x,y,z)$ for each $z = z_k$, for $z = z_1, \cdots, z_k$ may not be continuous along the z direction. We now apply another phase unwrapping operator, $\mathrm{unwrap}_z(\cdot)$ to get multi-slice B_z images as

$$B_z(x,y,z) = \mathrm{unwrap}_z\left(\widetilde{B_z}(x,y,z)\right) \text{ for } z = z_1, \cdots, z_K \quad (19)$$

To implement $\mathrm{unwrap}_z(\cdot)$, we examine any abrupt change of pixel values in multi-slice images of $\widetilde{B_z}$ along the z direction. Finding such an abrupt change, we add or subtract integer multiples of π to chosen slices of $\widetilde{B_z}$ images. Since this heuristic method may fail, we implemented a data verification procedure in CoReHA. Let m_i and τ_i be the average and standard deviation, respectively, of B_z data in the ith two-dimensional slice. If m_{i-1} and m_{i+1} belong to $[m_i - 3\tau_i,\ m_i + 3\tau_i]$ we calculate the three-dimensional Laplacian $\nabla^2 B_z$. Otherwise, we calculate the two-dimensional Laplacian $\nabla^2_{x,y} B_z$ dropping $\frac{\partial^2 B_z}{\partial z^2}$ in $\nabla^2 B_z$. As we mentioned in the previous section, since we find a scaled conductivity, we assume that this modification, if occur, does not affect much to a reconstructed scaled conductivity image.

C. Segmentation, electrode configuration and meshing

In order to reconstruct an image of σ, we should solve (11). Since data of $B_{z,1}$ and $B_{z,2}$ are now available, we need to compute the matrix A by solving the boundary value problem (13). In order to get the imaging domain Ω, we employ level-set based segmentation methods on each one of multi-slice magnitude images $M(x,y,z_k)$ for $k = 1, \cdots, K$. Caselles *et al.*, Chan and Vese, Xie and Mirmehdi and references therein explain basics of image segmentation methods [20-22].

Since the boundary of the imaging object in the MR magnitude image has weak edges and concave shapes, most of existing segmentation methods are not appropriate. We first use the statistically reinstating method (SRM) [23]. Based on a statistical variational formulation using local region information [24], SRM was developed to capture weak edges and concave shapes. After the boundary of the object including electrodes is segmented by SRM, we need additional manual work to segment the object without electrodes. This procedure using the level set is also a part of SRM and produces the extracted boundary of the object with electrode positions properly marked.

After segmenting the imaging domain, we need to generate its mesh to solve the forward problem using FEM and reconstruct conductivity images. In CoReHA, we use Triangle that is a well-known public-domain program provided with its source code [25].

D. Denoising and inpainting

Inside the imaging object, there may exist a local region where M in (15) is very small. This kind of MR signal void occurs in the outer layer of the bone, portions of lungs and gas-filled gastrointestinal organs or internal cavities. Following the noise analysis by Scott *et al.* and Sadleir *et al.* [26,27], the obtained B_z image becomes very noisy in such a defective region. Lee *et al.* suggested a PDE-based denoising method to reduce the noise level in B_z images [28]. Lee *et al.* also suggested a method called the harmonic inpainting where we replace the B_z data inside the local region of MR signal void by a synthetic data assuming a homogeneous conductivity inside the region [29]. For appropriate denoising and inpainting, further segmentation of internal regions may be necessary.

E. Numerical solution of forward problem and conductivity image reconstruction

We use FEM to solve both the forward problem in (13) and the conductivity image reconstruction problem in (11) with the boundary condition (14). Since we use a standard FEM for (13), we need a numerical differentiation of the solution u of (13) since $A[\sigma]$ consists of partial derivatives of u. Then, the computed ∇u has the first order accuracy with respect to the mesh size when the standard P_1 finite element is used. For the conductivity image reconstruction, we also used the standard P_1 finite element.

Ⅳ. DEMONSTRATION

Figure 2 shows a screen capture of CoReHA with its menu structure. In this section, we explain how to utilize CoReHA by showing results of key tasks needed for MREIT conductivity image reconstructions.

Figure 3(a)-(d) show an example of preprocessing including MR magnitude and phase image reconstructions using (16) and (17). Note that the phase image in (d) is wrapped within $\pm\pi$. By using the phase unwrapping and unit conversion in (18) and (19), we get the B_z image shown in (e). Figure 4(a) and (b) show the results of image segmentation for the extraction of object's boundary and electrode positions by using the level-set based methods. One can see the red line that is represented by the level-set information. Electrode positions are marked by using blue and yellow lines. Triangulation was

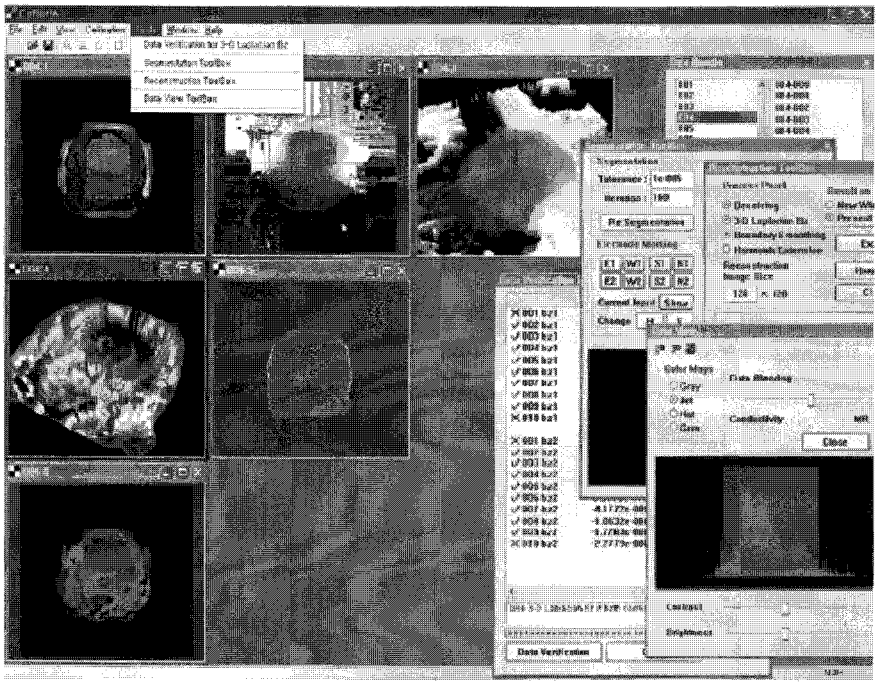

Fig. 2. Screen capture of CoReHA. It provides main menus for image viewing, calibration or coordinate setting and data processing including data verification, segmentation, meshing and image reconstruction.

applied to the segmented domain in (b) to produce the mesh shown in (c).

Figure 5 shows an example of the harmonic inpainting [29]. As illustrated in (a), we find the internal defective region where MR signal void occurred. For the case shown in Figure 5, the defective region includes two bones of a swine leg. From the B_z image before the harmonic inpainting in (b), we can see that the noise level is high in the defective region especially inside the outer layers of the bones. By using the inpainting method, we can produce a modified B_z image in (c) where we assumed that conductivity is constant inside the defective region. Figure 6(a) and (b) are reconstructed

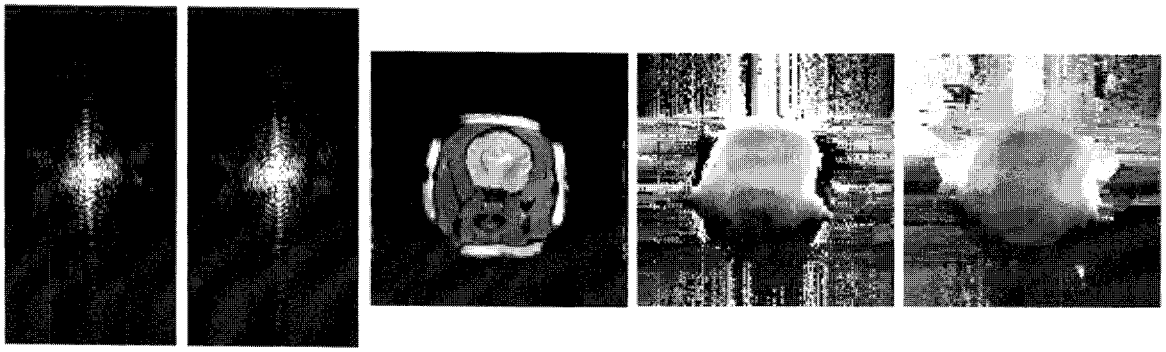

Fig. 3. (a) and (b) are k-space data from a canine head subject to a positive and negative injection current, respectively. (c) and (d) are reconstructed MR magnitude and phase image, respectively, by using the inverse Fourier transformation. (e) is B_z image. Imaging object is a canine head.

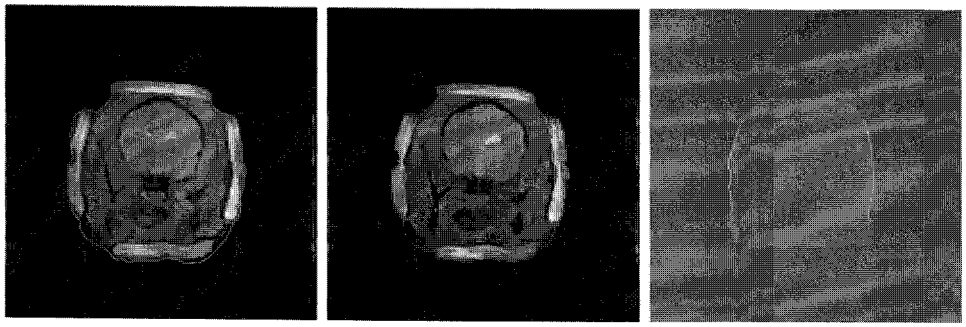

Fig. 4. (a) is the result of the boundary extraction using the statistically reinstating method (SRM) (Lee *et al.* 2007). (b) shows that electrode positions are marked after additional manual work using blue and yellow lines. (c) is the result of meshing using the triangulation. Imaging object is a canine head.

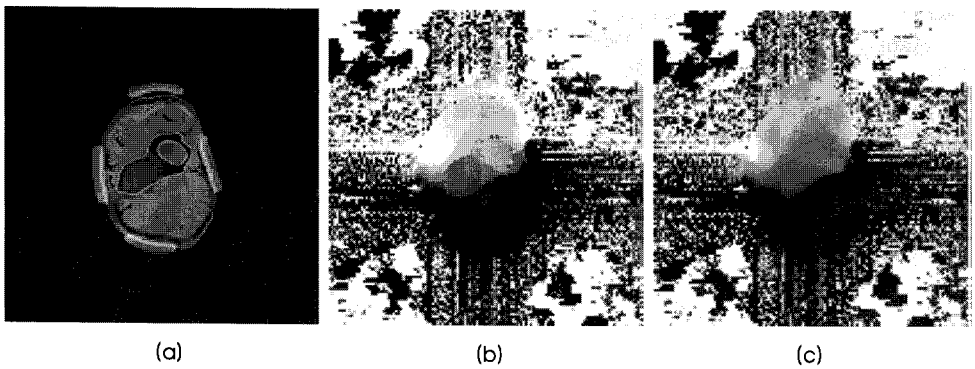

Fig. 5. (a) is the MR magnitude image with an internal defective region marked by orange lines. (b) and (c) are B_z images before and after the harmonic inpainting (Lee *et al.* 2006). Imaging object is a swine leg.

Fig. 6. (a) and (b) are reconstructed conductivity images using B_z data sets without and with applying the harmonic inpainting method, respectively. Imaging object is a swine leg.

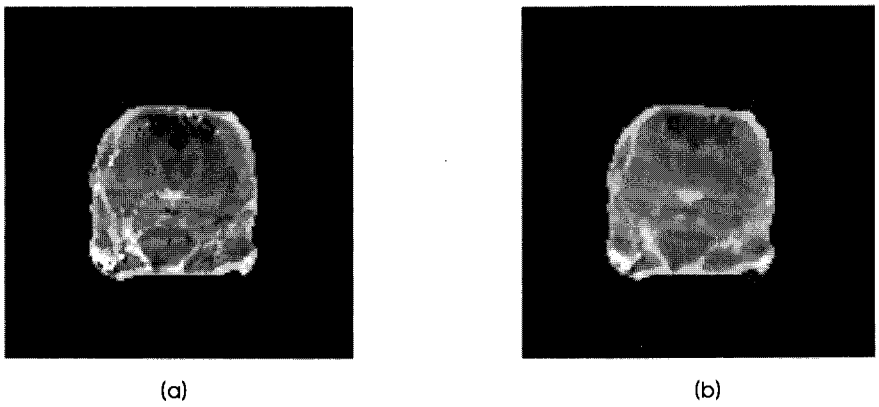

Fig. 7. (a) and (b) are reconstructed conductivity images using B_z data sets before and after applying the PDE-based denoising (Lee et al. 2005), respectively. Imaging object is a canine head.

conductivity images using B_z data sets before and after applying the harmonic inpainting method, respectively. In (b), the inpainting region is reconstructed to have one conductivity value even though spurious noise spikes shown in (a) are removed. We can also observe that the gap between two bones disappeared due to the choice of the inpainting region in Figure 5(a). These indicate that the harmonic inpainting must be used with care. Figure 7 shows typical results of the PDE-based denoising method [28]. We can see that the reconstructed conductivity image in (b) after using the denoising method is smoothed compared with the image in (a) that was obtained without applying the denoising method.

V. DISCUSSION AND CONCLUSION

This paper presents CoReHA, a software for MREIT conductivity image reconstructions. The software package is available for those who wish to reconstruct MREIT conductivity images using the harmonic B_z algorithm. It is expected to be a useful research tool for various MREIT studies of simulation, validation, animal and human imaging experiment and further technical development.

As described in this paper, numerical implementation of the harmonic B_z algorithm to process experimental MREIT data must be done in several steps. Since there exist various pitfalls in each step, special care must be given to avoid producing a wrong conductivity image. For example, image orientation or coordinate setting must be done properly and validated by using a test phantom. Otherwise, conductivity contrast in reconstructed images could have been reversed. When preprocessing methods such as the harmonic inpainting and denoising are adopted, their effects must be carefully examined based on concrete understanding of their limitations.

Future versions of the software will include implementations of other image reconstruction algorithms, more advanced numerical computations, better graphics and improved user

interface. In particular, we plan to implement the local harmonic B_z algorithm [13], ramp preserving denoising, image reconstruction using more than two current injections, sophisticated three-dimensional phase unwrapping, enhanced three-dimensional forward solver and visualization of current density distribution. Present version of CoReHA provides scaled conductivity images with contrast information only. Future version should be capable of producing absolute conductivity images.

REFERENCE

[1] N. Zhang, *Electrical Impedance Tomography based on Current Density Imaging*, Toronto, Canada: MS Thesis, Dept. of Elec. Eng, 1992.

[2] E.J. Woo, S.Y. Lee, and C.W. Mun, "Impedance tomography using internal current density distribution measured by nuclear magnetic resonance", *SPIE*, vol. 2299, pp. 377-385, 1994.

[3] O. Birgul, and Y.Z. Ider, "Use of the magnetic field generated by the internal distribution of injected currents for electrical impedance tomography", *Proc. IXth Int. Conf. Elec. Bio-Impedance*, Heidelberg, Germany, pp. 418-419, 1995.

[4] Y.Z. Ider, and O. Birgul, "Use of the magnetic field generated by the internal distribution of injected currents for electrical impedance tomography (MR-EIT)", *Elektrik*, vol. 6, pp. 215-225, 1998.

[5] O. Kwon, E.J. Woo, J.R. Yoon, and J.K. Seo, "Magnetic resonance electrical impedance tomography (MREIT): simulation study of J-substitution algorithm", *IEEE Trans. Biomed. Eng.*, vol. 49, pp. 160-167, 2002.

[6] E.J. Woo, J.K. Seo, and S.Y. Lee, "Magnetic resonance electrical impedance tomography (MREIT) in Holder D ed.", *Electrical Impedance Tomography: Methods, History and Applications*, Bristol, UK: IOP Publishing, 2005.

[7] E.J. Woo, and J.K. Seo, "Magnetic resonance electrical impedance tomography (MREIT) for high-resolution conductivity imaging", *Physiol. Meas.*, vol. 29, pp. R1-26, 2008.

[8] H.J. Kim, B.I. Lee, Y. Cho, Y.T. Kim, B.T. Kang, H.M. Park, S.Y. Lee, J.K. Seo, and E.J. Woo, "Conductivity imaging of canine brain using a 3 T MREIT system: postmortem experiments", *Physiol. Meas.*, vol. 28, pp. 1341-1353, 2007.

[9] H.J. Kim, T.I. Oh, Y.T. Kim, B.I. Lee, E.J. Woo, J.K. Seo, S.Y. Lee, O. Kwon, C. Park, B.T. Kang, and H.M. Park, "*In vivo* electrical conductivity imaging of a canine brain using a 3T MREIT system", *Physiol. Meas.*, vol. 29, pp. 1145-1155, 2008.

[10] T.S. Kim, B.I. Lee, C. Park, S.H. Lee, S.H. Tak, J.K. Seo, O. Kwon, and E.J. Woo, "A Matlab toolbox for magnetic resonance electrical impedance tomography (MREIT): MREIT toolbox", *IJBEM*, vol. 7, pp. 352-355, 2005.

[11] J.K. Seo, J.R. Yoon, E.J. Woo, and O. Kwon, "Reconstruction of conductivity and current density images using only one component of magnetic field measurements", *IEEE Trans. Biomed. Eng.*, vol. 50, pp. 1121-1124, 2003.

[12] S.H. Oh, B.I. Lee, E.J. Woo, S.Y. Lee, M.H. Cho, O. Kwon, and J.K. Seo, "Conductivity and current density image reconstruction using harmonic B_z algorithm in magnetic resonance electrical impedance tomography", *Phys. Med. Biol.*, vol. 48, pp. 3101-3116, 2003.

[13] J.K. Seo, S.W. Kim, S. Kim, J.J. Liu, E.J. Woo, K. Jeon, and C.O. Lee, "Local harmonic B_z algorithm with domain decomposition in MREIT: computer simulation study", *IEEE Trans. Med. Imag.*, vol. 27, pp. 1754-1761, 2008.

[14] O. Kwon, H.C. Pyo, J.K. Seo, and E.J. Woo, "Mathematical framework for B_z-based MREIT model in electrical impedance imaging", *Comp. Math. Appl.*, vol. 51, pp. 817-828, 2006.

[15] B.I. Lee, S.H. Oh, E.J. Woo, S.Y. Lee, M.H. Cho, O. Kwon, J.K. Seo, J.Y. Lee, and W.S. Baek, "Three-dimensional forward solver and its performance analysis in magnetic resonance electrical impedance tomography (MREIT) using recessed electrodes", *Phys. Med. Biol.*, vol. 48, pp. 1971-1986, 2003.

[16] T.I. Oh, Y. Cho, Y.K. Hwang, S.H. Oh, E.J. Woo, and S.Y. Lee, "Improved current source design to measure induced magnetic flux density distributions in MREIT", *J. Biomed. Eng. Res.*, vol. 27, pp. 30-37, 2006.

[17] OpenGL, http://www.opengl.org, 2008.

[18] M. Frigo and, S.G. Johnson, http://www.fftw.org, 2008.

[19] D.C. Ghiglia, and M.D. Pritt, "Two-Dimensional Phase Unwrapping: Theory, Algorithms and software", New York, USA: Wiley Interscience, 1998.

[20] V. Caselles, R. Kimmel, and G. Sapiro, "Geodesic active contours", *Int. J. Comput. Vis.*, vol 22, pp. 61-79, 1997.

[21] T. Chan, and L. Vese, "Active contours without edges", *IEEE Trans. Imag. Proc.*, vol. 10, pp. 266-277, 2001.

[22] X. Xie, and M. Mirmehdi, "RAGS: region-aided geometric snake", *IEEE Trans. Imag. Proc.*, vol. 13, pp. 640-652, 2004.

[23] C.O. Lee, S.H. Park, and J Hahn, "Method for image segmentation using statistically reinstating force and multi-resolution", Applied for Korea patent, 2007.

[24] S.H. Park, C.O. Lee, and J Hahn, "Image segmentation based on the statistical variational formulation using the local region information", *DAM Res. Rep.* 08-03, KAIST, Korea, 2008.

[25] J.R. Shewchuk, "Triangle: a two-dimensional quality mesh generator and Delaunay triangulator", http://www.cs.cmu.edu/$\sim$quake/triangle.html, 2005.

[26] G.C. Scott, M.L.G. Joy, R.L. Armstrong, and R.M. Hankelman, "Sensitivity of magnetic resonance current density imaging", *J. Magn. Reson.*, vol. 97, pp. 235-254, 1992.

[27] R. Sadleir, S. Grant, S.U. Zhang, B.I. Lee, H.C. Pyo, S.H. Oh, C. Park, E.J. Woo, S.Y. Lee, O. Kwon, and J.K. Seo, "Noise analysis in MREIT at 3 and 11 Tesla field strength", *Physiol. Meas.*, vol. 26, pp. 875-884, 2005.

[28] B.I. Lee, S.H. Lee, T.S. Kim, O. Kwon, E.J. Woo, and J.K. Seo, "Harmonic decomposition in PDE-based denoising technique for magnetic resonance electrical impedance tomography", *IEEE Trans. Biomed. Eng.*, vol. 52, pp. 1912-1920, 2005.

[29] S.H. Lee, J.K. Seo, C. Park, B.I. Lee, E.J. Woo, S.Y. Lee, O. Kwon, and J. Hahn, "Conductivity image reconstruction from defective data in MREIT: numerical simulation and animal experiment", *IEEE Trans. Med. Imag.*, vol. 25, pp. 168-176, 2006.